Excitons in InP/InAs inhomogeneous quantum dots

2003 J. Phys.: Condens. Matter 15 175

(http://iopscience.iop.org/0953-8984/15/2/317)

INSTITUTE OF PHYSICS PUBLISHING JOURNAL OF PHYSICS: CONDENSED MATTER

J. Phys.: Condens. Matter **15** (2003) 175–184 PII: S0953-8984(03)40027-1

Excitons in InP/InAs inhomogeneous quantum dots

E Assaid[1,2,4], E Feddi[2], J El Khamkhami[2] and F Dujardin[3]

[1] Groupe d'Optique et de Génie Physique du Solide, Faculté des Sciences, BP 20, El Jadida, Morocco
[2] Groupe d' Hétérostructures et Nanostructures de Semi-conducteurs, Ecole Normale Supérieure, BP 209, Martil, Tétouan, Morocco
[3] Institut de Physique et d'Electronique de Metz, 1 Boulevard Arago, 57078 Metz, France

E-mail: eassaid@hotmail.com

Received 29 July 2002, in final form 21 November 2002
Published 20 December 2002
Online at stacks.iop.org/JPhysCM/15/175

Abstract

Wannier excitons confined in an InP/InAs inhomogeneous quantum dot (IQD) have been studied theoretically in the framework of the effective mass approximation. A finite-depth potential well has been used to describe the effect of the quantum confinement in the InAs layer. The exciton binding energy has been determined using the Ritz variational method. The spatial correlation between the electron and the hole has been taken into account in the expression for the wavefunction. It has been shown that for a fixed size b of the IQD, the exciton binding energy depends strongly on the core radius a. Moreover, it became apparent that there are two critical values of the core radius, a_{crit} and a_{2D}, for which important changes of the exciton binding occur. The former critical value, a_{crit}, corresponds to a minimum of the exciton binding energy and may be used to distinguish between tridimensional confinement and bidimensional confinement. The latter critical value, a_{2D}, corresponds to a maximum of the exciton binding energy and to the most pronounced bidimensional character of the exciton.

1. Introduction

In the last two decades, the progress achieved in crystal growth techniques has enabled the fabrication of zero-dimensional (0D) nanoscale structures where the charge carriers are confined in the three directions of space. The class of 0D structures is composed of clusters, quantum crystallites (QC) and quantum dots (QDs). In this paper, we focus on homogeneous and inhomogeneous quantum dots (IQDs) with a spherical shape. The homogeneous quantum dots (HQDs) are semiconductor droplets embedded in a host matrix. They may be obtained by precipitation of a semiconductor in either an isolating [1] or a semiconducting [2, 3] matrix.

[4] Address for correspondence: Faculté des Sciences, Département de Physique, BP 20 El Jadida, Morocco.

They may also be synthesized as colloidal suspensions in organic liquids [4, 5]. The energy band gap of the host matrix is greater than that of the QD. The band offsets between the dot and the matrix materials give rise to confinement potentials of the charge carriers. Thus, electrons and holes are spatially localized and their energy levels are quantized and depend strongly on the size of the HQD.

For the last ten years, it has been possible to fabricate a new class of spherical QDs using a chemical growth process [6–8]. These spherical structures, called quantum dot–quantum wells (QDQWs) or IQDs, are grown layer by layer. In a first step, a spherical core of a semiconductor with a larger band gap is grown. The core plays the role of the substrate on which a thin spherical layer of a semiconductor with a smaller band gap is deposited. Finally, the whole structure is coated in a spherical shell of the semiconductor with the larger band gap. The final structure contains an internal nanoheterostructure with a quantum well inside the QD. As a consequence, electrons and holes are confined in the material with the smaller band gap. The whole structure presents a lot of similarities with quantum well systems.

Experimental investigations on different IQDs—ZnS(core, shell)/CdSe(well) [6], CdS/PbS [7], CdS/HgS [8], CdS/AgI, CdS/TiO_2 [9], ZnSe/CdSe [10] and ZnS/CdS [11]—have revealed outstanding and interesting properties. Indeed, due to the confinement of the charge carriers in the thin layer between the core and the shell, the absorption band edge is shifted to high energies and the luminescence efficiency is increased.

The theoretical studies which were devoted to IQDs have focused on the effect of the confinement in the middle well on single-particle energies. In this way, Kortan *et al* [6] have established the theory of the electronic structure in layered crystallites by means of approximations previously used for HQDs. Haus *et al* [12] have used a recursive method to determine the energies and the wavefunctions of free electrons and holes in multiple-shell structures. Taking into account the Coulomb potential energy and describing the confinement in a CdS/HgS/CdS structure by a finite-depth potential well, Schooss *et al* [13] have calculated theoretically the 1s–1s band-to-band transition energy.

In the last decade, there have been, to our knowledge, only a few theoretical studies which have focused on the properties of confined excitons in spherical or quasi-spherical QDs. Those focusing on the former were performed by Bryant [14]. This author extended the large-scale configuration interaction calculation, previously used in the study of multi-electrons and excitons in HQDs, to spherical CdS/HgS IQDs. He has shown that the thickness of the sandwiched layer has an important effect on the pair correlation in IQDs. He has also shown that the model of the screened pair interaction gives a good value of the exciton binding energy. A second study was performed by Wojs *et al* [15]. These authors studied the electronic structures of lens-shaped self-assembled QDs in the presence of a magnetic field. They have shown that the single-particle and exciton energies depend on the dot radius, the dot height, the confining potential depth and the magnetic field strength. A third study was performed by Ferreyra and Proetto [16]. These authors described the confinement in an IQD by means of an infinitely deep potential well; they took into account polarization charges, they neglected the coupling between the electron and the hole in the trial wavefunction and they considered the Coulomb interaction as a perturbation. They have shown that for a given size of the IQD, the exciton binding energy decreases monotonically when the core radius increases. In our previous study, we discussed the shortcomings of this model. Indeed, the model adopted by Ferreyra and Proetto gives results close to those from the model of a correlated pair confined in an infinitely deep potential only for the strong-confinement regime [17, 18]. A fourth study was performed by Kai Chang [19]. This author investigated the electronic structure of GaAs/$Ga_{1-x}Al_xAs$ IQDs. He showed that the electronic structure depends on the core-to-shell-radius ratio η. He has also shown that for a critical value of the ratio η, a type I–type

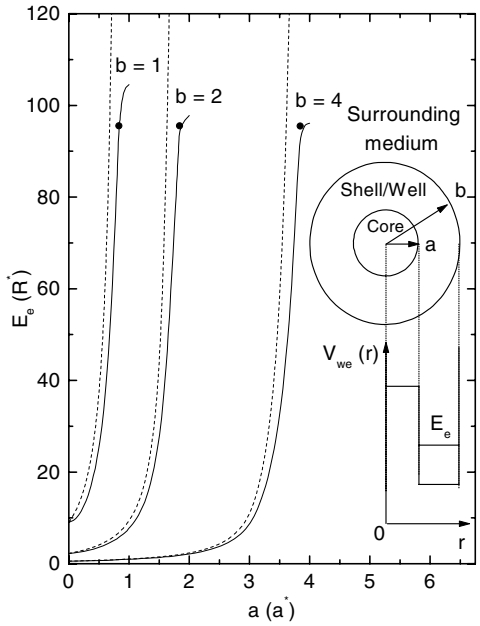

Figure 1. The electron ground state energy E_e versus the core radius a for three different values of the shell radius: $b = 1, 2$ and $4\ a^*$. The dots correspond to the electron critical values of the core radius a_{ce}. Inset: the schematic structure and the conduction band profile of the InP/InAs IQD.

II transition occurs. The author claimed that this transition may be observed by investigating experimentally the intensity of the photoluminescence peak for different IQD structures. The most recent study was made by El Khamkhami *et al* [17, 18]. These authors performed a variational determination of the exciton ground state energy in an IQD. They took into account the coupling between the electron and the hole in the trial wavefunction and determined the exciton ground state energy in the absence and in the presence of a uniform electric field. In the absence of the electric field, they showed that for the intermediate- and weak-confinement regimes and for a fixed size of the IQD, the exciton binding energy presents a minimum for a critical value of the core radius. They asserted that this critical value may be used to distinguish between tridimensional confinement and bidimensional confinement. They have also shown that in the presence of a uniform electric field, the Stark effect appears even for a small-size IQD in contrast to what happens in a HQD where the Stark effect appears only for large sizes.

In the present study, we consider an InP(core)/InAs(well/shell) IQD in water [13] or in an organic solution (see the inset of figure 1). We describe the junction between InP and InAs by means of finite-height barriers. We model the junction between InAs and the surrounding solution by infinite-height barriers. First, we determine analytically the ground state energies of an electron and a hole confined in the InAs layer. Then, we focus on the ground state energy of the 1s–1s exciton. We choose a variational wavefunction taking into account the Coulomb correlation between the electron and the hole and determine the exciton binding energy for weak, intermediate and strong confinements. The paper is divided into four sections. In section 2, we present the theory of the problem. In section 3, we discuss the essential results of the variational calculation. In section 4, we give our conclusions.

2. Ground state and binding energy

Let us consider an InP(core)/InAs(well/shell) IQD in water [13] or in an organic solution. The bottom of the InP conduction band is 0.4 eV above the bottom of the InAs conduction band [12]. The top of the InP valence band is 0.58 eV below the top of the InAs valence band [12]. Due to these band offsets, the probabilities of existence of an electron and a hole in the core are not equal to zero. For this reason, the junction between InP and InAs can be modelled by finite-height barriers (see the inset of figure 1).

The IQD as described above is composed of two materials with close dielectric constants ($\varepsilon_{\mathrm{InP}} = 12.1$, $\varepsilon_{\mathrm{InAs}} = 12.5$ [20]) embedded in a surrounding medium with a different dielectric constant ($\varepsilon_{\mathrm{H_2O}} = 1.78$ [13]). The dielectric discontinuity at the interface between the core and the shell may be ignored since the relative difference of the dielectric constant does not exceed 4%. The dielectric discontinuity at the interface between the shell and the surrounding medium gives rise to an image charge which slightly modifies the electron, hole and exciton energies. The contributions of the image charge to the free particle energies are: $-\sum_{l=0}^{\infty}(l+1)((\varepsilon/\varepsilon_{\mathrm{H_2O}})-1)r_i^{2l}b^{-2l-1}/\varepsilon(l(\varepsilon/\varepsilon_{\mathrm{H_2O}})+l+1)$, $i = \mathrm{e,h}$ [21]. e and h refer to the electron and the hole respectively. $\varepsilon = (\varepsilon_{\mathrm{InP}}+\varepsilon_{\mathrm{InAs}})/2$ is the dielectric constant over the whole IQD. The contribution of the image charge to the electron–hole interaction is: $-\sum_{l=0}^{\infty}(l+1)((\varepsilon/\varepsilon_{\mathrm{H_2O}})-1)r_{\mathrm{e}}^{l}r_{\mathrm{h}}^{l}b^{-2l-1}P_l(\cos\theta_{\mathrm{eh}})/\varepsilon(l(\varepsilon/\varepsilon_{\mathrm{H_2O}})+l+1)$ [21]. It is important to emphasize that each term of the sums given above is proportional to b^{-2l-1}. So the image charge contributions may be neglected as long as the shell radius b is greater than the bulk exciton Bohr radius, which corresponds to IQDs with common sizes.

In the framework of the effective mass approximation and assuming an isotropic, parabolic and non-degenerate band, the Hamiltonians of the single electron and the single hole are

$$H_i = \left(\frac{\hbar}{j}\nabla_i\right)\frac{1}{2m_i^*(r)}\left(\frac{\hbar}{j}\nabla_i\right) + V_{\mathrm{w}i} \qquad (i = \mathrm{e,h}). \tag{1}$$

The electron and hole effective masses are given in units of the free electron mass m_0:

$$m_i^*(r) = \begin{cases} m_{i1}^*, & r_i < a \ (i = \mathrm{e,h}) \\ m_{i2}^*, & a < r_i < b \ (i = \mathrm{e,h}). \end{cases} \tag{2}$$

a and b are respectively the core and the shell radii (see the inset of figure 1). The electron and hole confining potentials $V_{\mathrm{w}i}$ $(i = \mathrm{e,h})$ are expressed as follows:

$$V_{\mathrm{w}i} = \begin{cases} V_{0i}, & 0 < r_i < a \ (i = \mathrm{e,h}) \\ 0, & a < r_i < b \ (i = \mathrm{e,h}) \\ \infty, & b < r_i \ (i = \mathrm{e,h}). \end{cases} \tag{3}$$

In a first step, we focus on the effect of the penetration of the electron and hole wavefunctions in the core region. We neglect the effect of the effective mass mismatch at the junction between the core and the shell. We assume that the single-particle effective mass over the whole structure, m_i^* $(i = \mathrm{e,h})$, is equal to the average of the core and the shell effective masses: $\overline{m_i^*} = (m_{i1}^* + m_{i2}^*)/2$. Consequently, the electron and hole effective masses are respectively equal to 0.051 m_0 and 0.535 m_0 [12]. The influence of the effective mass mismatch will be discussed at the end of section 3.

Subsequently, we use as the unit of energy $R^* = \mu e^4/2\varepsilon^2\hbar^2 = 4.187$ meV, which is equal to the absolute value of the 3D exciton energy. We use as the unit of length $a^* = \varepsilon\hbar^2/\mu e^2 = 13.979$ nm, which represents the 3D exciton effective Bohr radius. μ is the reduced mass of the exciton. In these conditions, the single-particle Hamiltonians are

$$H_i = -\kappa_i\Delta_i + V_{\mathrm{w}i} \qquad (i = \mathrm{e,h}) \tag{4a}$$

where

$$\kappa_{\mathrm{e}} = \frac{1}{1+\sigma} \tag{4b}$$

and

$$\kappa_{\mathrm{h}} = \frac{\sigma}{1+\sigma}. \tag{4c}$$

σ is the electron-to-hole effective mass ratio ($\sigma = 0.0953$). The single-particle ground state energies and the associated wavefunctions are solutions of the Schrödinger equation:

$$H_i \Psi_i(r_i) = E_i \Psi_i(r_i) \qquad (i = \mathrm{e}, \mathrm{h}). \tag{5}$$

The last equation can be solved analytically; in order to determine its solutions one must consider three different cases for every value of the shell radius b. In the first case, the single-particle energy $E_i < V_{0i}$ and the core radius $a < a_{ci}$; the radial part of the single-particle wavefunction is

$$\Psi_i = \begin{cases} A_{1i}\dfrac{sh(k_{1i}r_i)}{r_i}, & 0 < r_i < a \ (i = \mathrm{e}, \mathrm{h}) \\ A_{2i}\dfrac{\sin(k_{2i}(r_i - b))}{r_i}, & a < r_i < b \ (i = \mathrm{e}, \mathrm{h}) \end{cases} \tag{6}$$

where $k_{1i} = \sqrt{(V_{0i} - E_i)/\kappa_i}$ and $k_{2i} = \sqrt{E_i/\kappa_i}$. In the second case, $E_i = V_{0i}$ and $a = a_{ci}$; the radial part of the single-particle wavefunction is

$$\Psi_i = \begin{cases} A_{3i}, & 0 < r_i < a \ (i = \mathrm{e}, \mathrm{h}) \\ A_{4i}\dfrac{\sin(k_{4i}(r_i - b))}{r_i}, & a < r_i < b \ (i = \mathrm{e}, \mathrm{h}) \end{cases} \tag{7}$$

where $k_{4i} = \sqrt{V_{0i}/\kappa_i}$. In the last case, $E_i > V_{0i}$ and $a > a_{ci}$; the radial part of the single-particle wavefunction is expressed as follows:

$$\Psi_i = \begin{cases} A_{5i}\dfrac{\sin(k_{5i}r_i)}{r_i}, & 0 < r_i < a \ (i = \mathrm{e}, \mathrm{h}) \\ A_{6i}\dfrac{\sin(k_{6i}(r_i - b))}{r_i}, & a < r_i < b \ (i = \mathrm{e}, \mathrm{h}) \end{cases} \tag{8}$$

where $k_{5i} = \sqrt{(E_i - V_{0i})/\kappa_i}$ and $k_{6i} = \sqrt{E_i/\kappa_i}$. In every case, the coefficients A_{ji} are determined by using the normalization condition and the continuity condition for the wavefunction at the point $r = a$. The energy E_i is obtained by using the continuity conditions for Ψ_i and $(1/m_i^*)(\mathrm{d}\Psi_i/\mathrm{d}r_i)$ at the point $r = a$. For a given value of the IQD radius, the transcendental equation giving the critical value of the core radius is

$$\left\{a\sqrt{V_{0i}/\kappa_i}\cot((a-b)\sqrt{V_{0i}/\kappa_i})\right\} - 1 = 0 \qquad (i = \mathrm{e}, \mathrm{h}). \tag{9}$$

Using the same units of length and energy as for the single particles, the exciton Hamiltonian is

$$H = H_{\mathrm{e}} + H_{\mathrm{h}} - \frac{2}{r_{\mathrm{eh}}}. \tag{10}$$

The ground state of the confined exciton presents spherical symmetry. Thus, the wavefunction describing this state must be expressed as a function of the distances r_{e}, r_{h} and r_{eh}. With these coordinates, the Laplacian operators are

$$\Delta_i = \frac{\partial^2}{\partial r_i^2} + \frac{2}{r_i}\frac{\partial}{\partial r_i} + \frac{r_i^2 - r_j^2 + r_{\mathrm{eh}}^2}{r_i r_{\mathrm{eh}}}\frac{\partial^2}{\partial r_i\,\partial r_{\mathrm{eh}}} + \frac{\partial^2}{\partial r_{\mathrm{eh}}^2} + \frac{2}{r_{\mathrm{eh}}}\frac{\partial}{\partial r_{\mathrm{eh}}} \qquad (i, j = \mathrm{e}, \mathrm{h} \text{ with } i \neq j). \tag{11}$$

The exciton ground state energy and the associated wavefunction are solutions of the effective Schrödinger equation:

$$H\Psi(r_e, r_h, r_{eh}) = E\Psi(r_e, r_h, r_{eh}). \tag{12}$$

This equation does not admit analytical solutions, so we have to determine its ground state solutions using an approximation method. In this paper, we opt for the variational principle. We choose the following trial wavefunction:

$$\Psi(r_e, r_h, r_{eh}) = \Psi_e(r_e)\Psi_h(r_h)\exp(-\alpha r_{eh}). \tag{13}$$

$\Psi_e(r_e)$ and $\Psi_h(r_h)$ are, respectively, the electron and hole wavefunctions. The exponential factor is introduced in order to take into account the Coulomb attraction between the electron and the hole. α is a variational parameter. The exciton ground state energy is obtained by minimization of the expectation value of H with respect to α:

$$E = \min_{\alpha} \frac{\langle\Psi|H|\Psi\rangle}{\langle\Psi|\Psi\rangle}. \tag{14}$$

Before closing this section, it is important to emphasize that for a given value of the IQD radius b, the exciton wavefunction (equation (13)) has three different expressions according to the core radius a. For $a < a_{ce}$, both $\Psi_e(r_e)$ and $\Psi_h(r_h)$ are given by equation (6). When the core radius a is between a_{ce} and a_{ch}, $\Psi_e(r_e)$ is given by equation (8) while $\Psi_h(r_h)$ is given by equation (6). Finally, for $a > a_{ch}$, both $\Psi_e(r_e)$ and $\Psi_h(r_h)$ are given by equation (8).

3. Results and discussion

First, we present the single-particle ground state energy as a function of the IQD parameters.

Figure 1 shows the variations of the electron ground state energy E_e against the core radius a for three different values of the shell radius b: $b = 1$, 2 and 4 a^* in the two cases of infinite and finite band offsets between InP and InAs. First, we remark that for a given size b of the IQD, E_e increases monotonically in both cases when a increases from 0 to b. In the case of infinite band offsets ($V_{0e} \to \infty$), the electron is supposed completely confined in the InAs well, its probability of existence in the core region is equal to zero and E_e is equal to $\pi^2/(1+\sigma)(b-a)^2$. In the case of finite band offsets ($V_{0e} = 95.525\ R^*$), the electron can slip away toward the core region. When a is equal to 0, the IQD is equivalent to an InAs HQD and E_e is equal to $\pi^2/(1+\sigma)b^2$. For a critical value of the core radius a equal to a_{ce}, E_e is equal to V_{0e}. When a is equal to b, the IQD reduces to an InP HQD and E_e is equal to $V_{0e} + \pi^2/(1+\sigma)b^2$. For values of the core radius a between 0 and a_{ce}, the electron energy lies in the interval $0 < E_e < V_{0e}$ and the oscillatory part of the electron wavefunction is confined in the InAs layer. For values of the core radius a between a_{ce} and b, E_e is greater than V_{0e} and the oscillatory part of the electron wavefunction is extended over the whole IQD.

With the intention of studying the influence of the reduction of the InAs thickness on the electron–hole correlation, we define the exciton binding energy as follows:

$$E_b = E_e + E_h - E_X. \tag{15}$$

Figure 2 shows the variations of the exciton binding energy E_b versus the ratio a/b for values of the shell radius b larger than or equal to 1 a^*: $b = 1$, 2 and 4 a^*. The full curves present the variational results obtained in the case of finite band offsets between the core and the shell of the structure ($V_{0e} = 95.525\ R^*$, $V_{0h} = 138.512\ R^*$). The dashed curves present the variational results obtained in the case of infinite band offsets between the core and the shell of the structure ($V_{0e} \to \infty$, $V_{0h} \to \infty$).

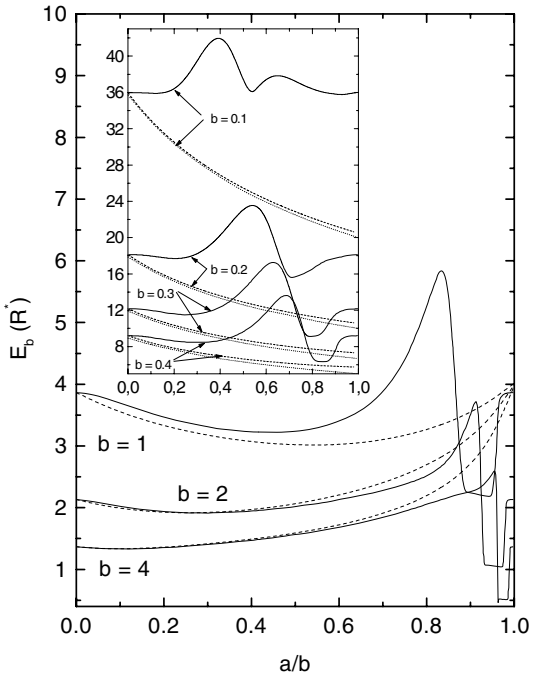

Figure 2. The exciton binding energy versus the ratio a/b for intermediate- and weak-confinement regimes ($b = 1$, 2 and 4 a^*). Inset: the exciton binding energy against the ratio a/b for the strong-confinement regime ($b = 0.1$, 0.2, 0.3 and 0.4 a^*).

In the case of infinite band offsets between InP and InAs, the exciton is supposed completely confined in the InAs layer. When a/b is equal to 0, the IQD is equivalent to an InAs HQD and the three curves corresponding to $b = 1$, 2 and 4 a^* tend respectively to the limits 3.86, 2.13 and 1.36 R^* which are in good agreement with the results obtained by Kayanuma [22, 23]. When a/b increases, the effect of the volume reduction leads to an enhancement of the kinetic energy and a diminution of the absolute value of the Coulomb potential energy. As a consequence, the exciton binding energy decreases. For a critical value $(a/b)_{\mathrm{crit}}$, there is an equilibrium between the effect of the volume reduction and the effect of the bidimensional confinement, so the exciton binding energy is minimal. When a/b increases from $(a/b)_{\mathrm{crit}}$ to unity, the InAs layer tends to become a spherical surface and the effect of the bidimensional confinement becomes predominant. As a consequence, the exciton binding energy increases. When a/b tends to 1, the exciton binding energy tends to 4 R^* which corresponds to the well-known two-dimensional exciton binding energy [24, 25].

In the case of finite band offsets between InP and InAs, the leakage of the exciton wavefunction toward the core region is no longer negligible, especially for the thin InAs layer. For a/b equal to 0, the IQD reduces to an InAs HQD. When a/b increases, the exciton binding energy decreases. For a critical value $(a/b)_{\mathrm{crit}}^{\mathrm{finite}}$, the exciton binding energy is minimal. When a/b varies from $(a/b)_{\mathrm{crit}}^{\mathrm{finite}}$ to $(a/b)_{2\mathrm{D}}$, the exciton binding energy increases. For a value of the ratio a/b equal to $(a/b)_{2\mathrm{D}}$, both the electrons and the holes are confined in a thin InAs layer; the exciton presents a bidimensional character and its binding energy is maximal. When a/b increases from $(a/b)_{2\mathrm{D}}$ to a_{ce}/b, the exciton binding energy decreases. For a/b equal to a_{ce}/b, the electron is no longer confined in the InAs layer and the oscillatory part of its

wavefunction is extended over the entire IQD. For a structure such as $a_{ce}/b \leqslant a/b \leqslant a_{ch}/b$, the oscillatory part of the electron wavefunction is extended over the whole IQD while the oscillatory part of the hole wavefunction is localized in the InAs layer; the exciton behaves like a non-correlated electron–hole pair and the exciton binding energy is quasi-constant. When a/b is equal to a_{ch}/b, the hole is no longer confined in the InAs layer and the oscillatory part of its wavefunction is extended over the entire IQD. For a structure such as $a_{ch}/b < a/b < 1$, the exciton binding energy increases. When a/b is equal to 1, the IQD reduces to an InP HQD.

The inset of figure 2 presents the variations of the exciton binding energy E_b as a function of the ratio a/b for values of the shell radius b smaller than 1 a^*: $b = 0.1$, 0.2, 0.3 and 0.4 a^*. The full curves represent the variational results obtained in the case of finite band offsets between InP and InAs. The dashed curves represent the variational results obtained in the case of infinite band offsets between InP and InAs. The dotted curves represent the results obtained by Ferreyra and Proetto [16] using the perturbation approach.

In the case of the perturbation method, the exciton is treated as a non-correlated electron–hole pair completely confined in the InAs layer. We begin by analysing two particular cases: $a = 0$ and b. In the former case, the nanostructure is equivalent to an HQD with a radius equal to b; the kinetic energy gives the leading contribution to the total energy: $\langle T\rangle = \pi^2/b^2$, $\langle V\rangle = -3.572/b$ and $\langle H\rangle = \pi^2/b^2 - 3.572/b$. In the second case, the nanostructure is equivalent to a small spherical surface with a radius equal to b; the Coulomb energy gives the leading contribution to the total energy: $\langle T\rangle = 0$, $\langle V\rangle = -2/b$ and $\langle H\rangle = -2/b$. Thus, the exciton binding energy decreases monotonically from the $3.572/b$ limit to the $2/b$ limit when a/b increases from 0 to 1 [17, 18].

In the case of the variational method with infinite band offsets between InP and InAs, the exciton is treated as a correlated electron–hole pair completely confined in the InAs layer. When a/b is equal to 0, the IQD is equivalent to an InAs HQD and the four curves corresponding to $b = 0.1$, 0.2, 0.3 and 0.4 a^* tend respectively to the limits 35.97, 18.11, 12.16 and 9.19 R^*. These last values are in good agreement with the results obtained by Kayanuma [22, 23]. When a/b increases, the volume of the structure becomes less important. As a consequence, the exciton binding energy decreases. When a/b tends to 1, the IQD is equivalent to a small spherical surface of InAs. The four curves corresponding to $b = 0.1$, 0.2, 0.3 and 0.4 a^* tend respectively to the limits 20.63, 10.61, 7.32 and 5.74 R^* [24].

In the case of the variational method with finite band offsets between InP and InAs, the exciton is treated as a correlated electron–hole pair incompletely confined in the InAs layer. Thus, one or both of the particles can slip away toward the core region. The exciton binding energy generally presents two minima and one maximum. For a/b equal to 0, the IQD is equivalent to an InAs HQD. When a/b increases, the effect of the tridimensional confinement decreases. As a result, the exciton binding energy decreases. When a/b is equal to $(a/b)_{crit}^{finite}$, the exciton binding energy is minimal. For a structure such as $(a/b)_{crit}^{finite} < a/b < (a/b)_{2D}$, the exciton binding energy increases. When a/b is equal to $(a/b)_{2D}$, the exciton binding energy is maximal. For $a/b > (a/b)_{2D}$, the exciton binding energy decreases until a minimal value is reached. When a/b is equal to 1, the IQD reduces to an InP HQD.

We now discuss the influence of the effective mass mismatch on the exciton binding energy. We use the following data: $m_{e1}^* = 0.079\, m_0$, $m_{e2}^* = 0.023\, m_0$, $m_{h1}^* = 0.65\, m_0$ and $m_{h2}^* = 0.42\, m_0$ [12]. Figure 3 shows the variations of the exciton binding energy E_b as a function of the ratio a/b for three different values of b: $b = 1$, 2 and 4 a^*. The full curves present the variational results with the effective mass mismatch effect. The dashed curves present the variational results without the effective mass mismatch effect. We remark that the curves appear nearly the same, so the conclusions drawn from figure 2 remain valid. The differences between the two cases lie in two essential points: in the presence of the effective

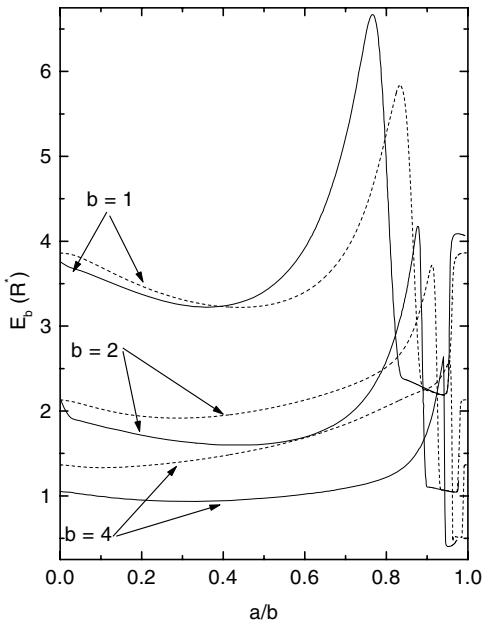

Figure 3. The exciton binding energy versus the ratio a/b for intermediate- and weak-confinement regimes with and without the effective mass mismatch effect.

mass mismatch effect, (i) the maxima of the curves are more pronounced and (ii) the plateaus are larger. The former observation is a consequence of the fact that for a thin InAs layer, the electron-to-hole effective mass ratio is smaller ($\sigma_{\mathrm{InAs}} = 0.0547$). The second observation is due to the fact that the range of a/b for which the exciton is separated is larger.

Up to now, there has been, to our knowledge, only one experimental study devoted to InAs/InP IQDs [26]. In this study, the core plays the role of the well and the shell plays the role of the barrier. On the other hand, there are no experimental data relating to InP/InAs IQDs. The core (barrier)/shell (well) system abundantly studied experimentally is the CdS/HgS system. In [27], Mews *et al* have investigated the absorption and fluorescence spectra of CdS/HgS IQDs by transient hole burning and fluorescence line narrowing spectroscopy. According to this study, the CdS/HgS IQDs with core and shell radii equal respectively to 2.35 and 2.65 nm exhibit a band gap $E_{\mathrm{g}} = 2.63$ eV. The model taking into account the effective mass mismatch used in the present study gives for the same IQD a theoretical value of the effective band gap $E_{\mathrm{g}}^{\mathrm{th}} = 2.89$ eV. This IQD is capped by one monolayer of CdS in order to passivate its surface and to eliminate surface effects [27]. The measurement of the exciton total energy leads to the experimental value $E_{\mathrm{T}} = 1625$ meV [14]. The model used in the present work gives a theoretical value of the exciton total energy $E_{\mathrm{T}}^{\mathrm{th}} = 1586$ meV.

4. Conclusions

In conclusion, we have studied theoretically the electronic structure of an InP/InAs IQD in the framework of the effective mass approximation. We have modelled the junction between InP and InAs by finite-height barriers. We have determined analytically the ground state energies of an electron and a hole confined in the IQD. We have shown that for a given value of the IQD radius, the single-particle energies increase monotonically when the core radius increases.

This property may be exploited in order to design IQDs with a predefined effective gap. We have also studied the ground state of an exciton confined in the IQD. We have determined the ground state energy by means of the Ritz variational method. We have shown that the 1s–1s exciton binding energy is dependent on the core-to-shell-radius ratio. For a given value b of the IQD radius, we have brought attention to the existence of two critical values of the core radius for which significant changes of the exciton binding energy take place. The first critical value, $a_{\text{crit}}^{\text{finite}}$, corresponds to a minimum of the exciton binding energy and may be used to distinguish between tridimensional confinement and bidimensional confinement. The second critical value, $a_{2\text{D}}$, corresponds to a maximum of the exciton binding energy and to the most pronounced bidimensional character of the IQD. Some preliminary calculations that we have performed show that IQDs with a pronounced bidimensional character ($a/b = (a/b)_{2\text{D}}$) present outstanding optical properties, i.e. a great oscillator strength and a very short lifetime of the confined exciton. These calculations also show that the oscillator strength decreases drastically for the range of sizes for which the exciton is spatially separated ($a_{\text{ce}} < a < a_{\text{ch}}$). Finally, we hope that the present study will allow a better understanding of the behaviour of excitons confined in IQDs.

References

[1] Ekimov A I, Kudryavtsev I A, Ivanov M G and Efros A L 1990 *J. Lumin.* **46** 83
[2] Yoffe A D 1993 *Adv. Phys.* **42** 173
[3] Yoffe A D 2001 *Adv. Phys.* **50** 1
[4] Murakoshi K, Hosokawa H, Saitoh M, Wada Y, Sakata T, Mori H, Satoh M and Yanagida S 1998 *J. Chem. Soc., Faraday Trans.* **4** 579
[5] Hambrock J, Birkner A and Fisher R A 2001 *J. Mater. Chem.* **11** 3197
[6] Kortan A R, Hull R, Opila R L, Bawendi M G, Steigerwald M L, Carroll P J and Brus L 1990 *J. Am. Chem. Soc.* **112** 1327
[7] Zhou H S, Honma I and Komiyama H 1993 *J. Phys. Chem.* **97** 895
[8] Mews A, Eychmuller A, Giersig M, Schooss D and Weller H 1994 *J. Phys. Chem.* **98** 934
[9] Spanhel L, Weller H and Henglein A 1994 *J. Am. Chem. Soc.* **109** 6632
[10] Hoener C F, Allan K A, Brad A J, Campion A, Fox M A, Mallouk T E, Webber S E and White J M 1992 *J. Phys. Chem.* **96** 3812
[11] Little R B, El-Sayed M A, Bryant G W and Burke S 2001 *J. Chem. Phys.* **114** 1813
[12] Haus J W, Zhou H S, Honma I and Komiyama H 1993 *Phys. Rev.* B **47** 1359
[13] Schooss D, Mews A, Eychmuller A and Weller H 1994 *Phys. Rev.* B **49** 17072
[14] Bryant G B 1995 *Phys. Rev.* B **52** R16997
[15] Wojs A, Hawrylak P, Fafard S and Jacak L 1996 *Phys. Rev.* B **54** 5604
[16] Ferreyra J M and Proetto C R 1998 *Phys. Rev.* B **57** 9061
[17] El Khamkhami J, Feddi E, Assaid E, Dujardin F, Stébé B and Diouri J 2002 *Physica* E **15** 99
[18] El Khamkhami J, Feddi E, Assaid E, Dujardin F, Stébé B and Diouri J 2001 *Phys. Low-Dim. Struct.* **9/10** 131
[19] Chang K 2000 *Phys. Rev.* B **61** 4743
[20] Mathieu H 1987 *Physique des Semi-Conducteurs et des Composants Électroniques* (Paris: Masson)
[21] Brus L 1984 *J. Chem. Phys.* **80** 4403
[22] Kayanuma Y 1986 *Solid State Commun.* **59** 405
[23] Kayanuma Y 1988 *Phys. Rev.* B **38** 9797
[24] Kayanuma Y and Saito N 1992 *Solid State Commun.* **84** 771
[25] Le Goff S and Stébé B 1992 *J. Phys. B: At. Mol. Opt. Phys.* **25** 5261
[26] Cao Y W and Banin U 1999 *Angew. Chem. Int. Edn* **38** 3692
[27] Mews A, Kadavanich A V, Banin U and Alivisatos A P 1996 *Phys. Rev.* B **53** R13242